Published in final edited form as:
Biomaterials. 2012 October ; 33(28): 6783–6792. doi:10.1016/j.biomaterials.2012.05.068.

Polymeric Multilayers that Localize the Release of Chlorhexidine from Biologic Wound Dressings

Ankit Agarwal[1], **Tyler B. Nelson**[1], **Patricia R. Kierski**[2], **Michael J. Schurr**[3], **Christopher J. Murphy**[4], **Charles J. Czuprynski**[5,*], **Jonathan F. McAnulty**[2,*], and **Nicholas L. Abbott**[1,*]

[1]Department of Chemical and Biological Engineering, University of Wisconsin-Madison

[2]Department of Surgical Sciences, School of Veterinary Medicine, University of Wisconsin-Madison

[3]Department of Surgery, School of Medicine, University of Colorado-Denver

[4]Department of Surgical and Radiological Sciences, School of Veterinary Medicine, University of California-Davis

[5]Department of Pathobiological Sciences, School of Veterinary Medicine, University of Wisconsin-Madison

Abstract

Biologic wound dressings contain animal-derived components and are susceptible to high infection rates. To address this issue, we report an approach that permits incorporation of non-toxic levels of the small-molecule antiseptic ‘chlorhexidine’ into biologic dressings. The approach relies on the fabrication of polyelectrolyte multilayer (PEMs) films containing poly(allylaminehydrochloride) (PAH), poly(acrylicacid) (PAA), and chlorhexidine acetate (CX) on elastomeric poly(dimethylsiloxane) (PDMS) sheets. The PEMs (20-100 nm thick) are subsequently stamped onto the wound-contact surface of a synthetic biologic dressing, Biobrane, which contains collagen peptides. Chlorhexidine loading in the PEMs was tailored by tuning the number of (CX/PAA) bilayers deposited, providing burst release of up to 0.98±0.06 μg/cm^2 of CX over 24 h, followed by zero order release of 0.35±0.04 μg/cm^2/day for another week. Although the CX concentrations released were below the reported *in vitro* cytotoxicity limit (5 μg/mL over 24 h) for human dermal fibroblasts, they killed 4 $\log_{10}$ counts of pathogenic bacteria *Staphylococcus aureus* in solution. The CX/PEMs could be stamped onto Biobrane with high efficiency to provide CX release kinetics and *in-vitro* antibacterial activity similar to that on PDMS stamps. In a full-thickness ‘splinted’ dermal wound-model in normal wild-type mice, the CX-functionalized Biobrane showed no decrease in either its adherence to the wound-bed or wound-closure rate over 14 days. The murine wounds topically inoculated with ~10^5 CFU/cm^2 of

*Corresponding authors: Prof. N. L. Abbott, PhD Department of Chemical and Biological Engineering, University of Wisconsin 1415 Engineering Drive, Madison, WI 53706 (USA) abbott@engr.wisc.edu Prof. J. F. McAnulty, DVM, PhD Department of Surgical Sciences, School of Veterinary Medicine, University of Wisconsin 2015 Linden Drive, Madison, WI 53706 (USA) mcanultj@svm.vetmed.wisc.edu Prof. C. J. Czuprynski, PhD Department of Pathobiological Sciences, School of Veterinary Medicine, University of Wisconsin 2015 Linden Drive, Madison, WI 53706 (USA) czuprync@svm.vetmed.wisc.edu.

Supporting Information is available online or from the authors. AA, MJS, CJC, CJM, JFM, and NLA possess financial interests in Wound Engineering LLC and/or Imbed Biosciences Inc, for-profit organizations that have filed patent applications and/or are commercializing aspects of the work reported in this publication.

S. aureus and treated with CX-functionalized Biobrane demonstrated a 3 $\log_{10}$ decrease in the wound's bacterial burden within 3 days, compared to persistent bacterial colonization found in wounds treated with unmodified Biobrane (n=10 mice, $p<0.005$). Overall, this study presents a promising approach to prevent bacterial colonization in wounds under biologic dressings.

Keywords

Polyelectrolye multilayers; chlorhexidine; wound; dressing; mice; antimicrobial

1. INTRODUCTION

Biologic wound dressings that contain animal-derived components, such as collagen peptides and extra-cellular matrix proteins, represent an important advance in wound care as they have been shown to lead to superior healing rates [1, 2]. These dressings integrate into surgically-prepared wound-beds, minimizing dead space for bacterial proliferation and acting as a temporary skin-substitute. The dressings provide a scaffold for tissue regeneration and a barrier to exogenous bacteria, while soothing nerve endings to reduce pain. However, even low levels of bacterial colonization endogenous to the wound-bed under biologic dressings frequently leads to clinical infections. This results in an undesirably high rate of dressing loss from the patient (10-20%), and restricts the use of biologic dressings to a limited range of wound indications [3-9]. Incorporation of broad spectrum antimicrobial agents into biologic dressings, engineered to result in localized release of antimicrobial agent(s) at non-toxic levels in the wounds while achieving adequate control of microbial burden, would reduce the incidence of microbial infections and enable the use of biologic dressings to manage a broader range of dermal wounds.

Chlorhexidine (CX) is a promising candidate antimicrobial agent for incorporation into wound dressings. It is considered the “gold standard” antiseptic that is active against gram-positive/gram-negative bacteria, facultative anaerobes/aerobes, molds, yeasts and viruses [10]. It exhibits immediate bactericidal effect and has an excellent residual effect, which prevents reestablishment of microorganisms on the skin [11-13]. CX exerts antimicrobial activity through its positive charge at physiological pH, which destabilizes bacterial cell walls and alters bacterial osmotic equilibrium [14, 15]. These events result in precipitation of cytoplasmic contents and trigger microbial cell death [16]. In clinical practice, 0.05% (=500 μg/mL) CX solutions or 0.2% w/w CX creams are used as topical formulations for cleansing and antisepsis of skin, burns and dermal wounds [13, 17-19]. Recently, dressings containing 25-500 mg of CX (releasing >50 μg/mL CX per hr) were approved by the U.S. Food and Drug Administration (FDA) to disinfect skin surrounding intravenous catheter injection sites and prevent blood stream infections from microbes on the skin [19]. However, these formulations release CX concentrations that are at least 100 times higher than those shown to be cytotoxic *in vitro* to mammalian cell types present in the wound-bed [20, 21]. The use of CX formulations, therefore, has been limited solely to skin cleansing with short-term wound treatments. Additional studies have shown that CX concentrations ≥ 0.001% (=10 μg/mL) significantly decreased the viability of primary human dermal fibroblasts *in vitro* after a 24 h incubation, while a 0.0025% (=25 μg/mL) solution resulted in total cell death [22]. To address this toxicity problem, herein we report the use of nanometer-thick polymeric films to locally deliver non-toxic concentrations of CX from biologic dressings and inhibit bacterial colonization in dermal wounds.

The approach reported in this paper is based on functionalization of the wound-contact surface of biologic dressings with antibacterial nanofilms containing CX. The nanofilms used are polyelectrolyte multilayers (PEMs) fabricated by the ‘layer-by-layer’ assembly of

oppositely charged polymers of poly(allylamine hydrochloride) (PAH) and poly(acrylic acid) (PAA), and cationic chlorhexidine acetate, as illustrated in **Fig. 1**. PEMs are self-assembled, highly interpenetrated ultrathin nanocomposite films, typically with a thickness much less than 1 μm [23]. Their porous and supramolecular architecture allows incorporation of a broad range of bioactive molecules [24-26]. We hypothesized that PEMs could serve as a nanometer-thick matrix for spatial confinement and localized delivery of CX at the surface of biologic wound dressings. The functionalized biologic dressings which, as noted above, become integrated into the wound-bed to minimize dead space or fluid pockets, would thus allow localized release of CX from the PEMs directly at the site of microbial colonization on the wound-bed. We hypothesize that this localize release would significantly minimize the loading of CX needed to exert antibacterial activity, thus reducing systemic exposure and local cytotoxicity. We emphasize that this approach differs from conventional wound dressings (non-biologic) that are impregnated uniformly with sufficiently high quantities of antibacterial agents to achieve mass transport across wound fluid and thereby exert antibacterial activity on the wound-bed [19, 27, 28]. Notably, these high loadings of antibacterial agents have been documented to result in undesirable impairment of wound healing due to cytotoxicity [29, 30]. The concept of nanoscopic localization of CX within a PEM, as explored in this paper, builds from our previous *in-vitro* study in which PEMs containing silver-nanoparticles were deposited onto skin-dermis and determined to release non-cytotoxic concentrations of silver that killed bacteria in solution [31]. In this report, we test the proposition that PEMs releasing non-cytotoxic loadings of the cationic small molecule antiseptic CX can be integrated onto the wound-contact surface of biologic dressings to achieve antimicrobial activity in wounds.

Fabrication of PEMs requires multiple dipping, spraying, or rinsing cycles that expose a substrate to non-physiological solutions. Therefore, to avoid exposing biologic dressings to laborious chemical processing, we adopted the approach of fabricating PEMs on elastomeric polydimethylsiloxane (PDMS) substrates and then stamping the pre-formed PEMs onto the biologic dressings [32-34]. The approach involves incorporating a monolayer of micrometer-sized (1-2 μm) polystyrene beads within the nanometer-thick PEMs (as illustrated in **Fig. 1c)**. The polystyrene microspheres assist in transfer of PEMs onto the mechanically soft biologic dressing, as described in our previous report [34]. This approach has an additional meritorious attribute; it allows preferential spatial placement of PEMs (or multiple stamping of distinct bioactive PEMs) on the surface of the dressing.

In our study, we used Biobrane as an exemplar of a biologic dressing. Biobrane is widely used in hospitals to treat first and second degree pediatric burns [8]. It is constructed of a thin silicone sheet that is partially embedded with a nylon fabric onto which purified peptides from porcine dermal collagen are chemically bonded [35]. Blood and plasma clot in the collagen-coated nylon matrix, thereby firmly adhering the dressing to the wound until reepithelialization occurs. Bacterial proliferation is minimized, in part, by reducing the development of fluid pockets under the dressing [35]. Clinical studies, however, have shown high rates of infection under Biobrane, leading to loss or need for removal of 10-20% of the dressings applied to wounds [4-8, 36]. This study demonstrates that nanoscopic localization of CX on the wound-contact surface of biologic dressings such as Biobrane can significantly lower the microbial colonization in wounds, preventing incidence of microbial infections under the biologic dressings while significantly improving the margin of safety related to the cytotoxicity of topical CX formulations.

2. MATERIALS AND METHODS

2.1 Materials

PAA (Mw= 60 kDa) was obtained from Polysciences (Warrington, PA). PAH (Mw= 70 kDa), Chlorhexidine diacetate (CX) (Mw= 625 Da) and all other reagents were obtained from Sigma Aldrich (St. Louis, MO). Wound dressing Biobrane® was purchased from UDL Labs, Rockford, IL. Glass microscope slides (Fisher Scientific, Pittsburgh, PA) and silicon wafers (Silicon Sense, Nashua, NH) were cleaned sequentially in piranha solution [70:30 (% v/v) H_2SO_4:H_2O_2] and alkaline solution (70:30 (% v/v) KOH:H_2O_2) for 1 h at ~80 °C, according to published procedures [37]. If required, cleaned glass slides were coated with octadecyltrichlorosilane (OTS) as described earlier [38] to generate a low-energy hydrophobic surface.

2.2 Preparation of PEMs

Poly(dimethylsiloxane) (PDMS) stamps were fabricated by curing Sylgard 184 (10:1 base to catalyst; Dow Chemical, Midland, MI) on top of OTS-coated glass slides at 60°C for 24 h. After curing, PDMS stamps were released from the glass slides and PEMs were assembled on the face of the stamps previously in contact with the OTS-coated glass. OTS-coated glass was used to ensure formation of a smooth surface on the PDMS stamps. PEMs with desired number of multilayers were assembled on PDMS stamps using a StratoSequence Robot (nanoStrata Inc, Tallahassee, FL), by sequential incubation in solutions of PAA and PAH (0.01 M by repeat unit) and/or chlorhexidine diacetate (0.1mM) for 10 min each. Polyelectrolytes solutions were adjusted to the desired pH using either 1 M HCL or 1 M NaOH. The formation of the PEMs onto PDMS was initiated by the adsorption of PAH. Stamps were rinsed with DI water 3 times for 1 min each after immersion in each polyelectrolyte solution. After assembly, the PEMs were dried in vacuum at 60°C for 1 h.

PAH labeled with fluorescein-5-isothiocyanate (FITC) (Ext/Em- 488/510) (cat# F1906, Invitrogen, Carlsbad, CA) using procedures described elsewhere [39] was used to prepare fluorescent films. Crimson fluorescent (Ext/Em- 625/645) FluoSpheres® carboxylate-modified polystyrene (PS) microspheres, 2 μm in diameter (cat# F8816, Invitrogen), or non-fluorescent carboxyl latex microspheres, 2 μm in diameter (cat# C37274, Invitrogen) were used to prepare PEMs containing microspheres. The microspheres were washed three times with DI water in Eppendorf tubes by centrifuging for 5 min at 9000g, and re-suspended in fresh DI water by sonication and vortexing before use. To deposit a monolayer of microspheres on the PEMs, PAH/PAA multilayers ending in cationic PAH layer were incubated with a suspension of negatively charged microspheres for 2 h, and then washed 3x with water [34]. Additional layers of polyelectrolytes were assembled subsequently over the microspheres.

2.3 Characterization of PEMs

An Olympus IX70 inverted microscope equipped with Chroma Technology Corp. (Rockingham, VT) fluorescence filter cubes was used to image the fluorescence from fluorescent PAH or PS microspheres. Images were captured and analyzed using the Metavue version 7.1.2.0 software package (Molecular Devices, Toronto, Canada). A Gaertner LSE ellipsometer (λ=632.8 nm, ψ=70°) was used to measure the thickness of PEMs prepared on the piranha cleaned and plasma oxidized silicon wafers (using PlasmaTherm 1441 RIE Instrument; 8 sccm O2, 20 s, 100 W). The effective substrate parameters (n_s= 3.85, k_s= -0.02) were measured by averaging six measurements on six different silicon-wafer pieces. The refractive index of the polymers was assumed to be 1.55 [40].

2.4 Chlorhexidine Release

Concentration of chlorhexidine in aqueous solutions was quantified by measuring their UV absorbance at 255 nm wavelength on a UV-Vis spectrophotometer (Beckman Coulter, Fullerton, CA)[27, 41]. Fresh standard calibration curves of CX concentrations in solution were prepared for each experiment, with 0.1 μg/mL CX used as minimum standard concentration. To determine the release profile of chlorhexidine in solution from PEMs, substrates containing PEMs were carved out into 2 cm diameter pieces and incubated with 2 mL PBS buffer (pH 7.4) in a 12-well (non-tissue culture treated) polystyrene plate. At defined time points, the entire solution was collected from the wells of the plate and replaced with fresh buffer. The samples were stored at 4°C until characterized. The raw data in μg/mL of the chlorhexidine concentration in the eluted solution was multiplied the total elution volume and normalized by the surface area of the substrate to be reported as drug released per unit surface area ($\mu g/cm^2$).

2.5 Antibacterial activity

The strain of *Staphylococcus aureus* subsp. *aureus* ATCC 25923 was obtained from The American Type Culture Collection (Manassas, VA). Bacteria were grown in Tryptic Soy Broth with Yeast Extract (BD, Franklin Lakes, NJ) overnight at 37°C with shaking (200 rpm) until a cell density of approximately 4×10^9 CFU/mL was reached, as determined from optical density (600 nm) measured on a UV–vis spectrometer (Beckman Coulter, Fullerton, CA). The bacterial suspensions were centrifuged at 2700 rpm for 10 min and the pellet washed and resuspended in PBS. In antibacterial assays, test substrates were placed in the wells of 96-well plates and incubated with 100 μL HBSS (Hank's Buffered Salt Solution) (pH 7.4) containing 10^7 CFU of *S. aureus*. Plates were incubated with shaking (200 rpm) at 37°C for 24 h. After incubation, the fluid in each well was collected, the wells rinsed twice with 200 μL ice cold PBS, and the fluid and washes from each well pooled and brought to 1 mL in PBS. Serial dilutions of the solutions in PBS were spread onto Trypticase Soy Blood Agar plates (#221261, BD, Franklin Lakes, NJ) and incubated at 37°C[31]. Viable bacterial colonies were counted on agar plates after 24 h incubation. All assays were carried out on at least three different days, with at 3-6 replicates of each test sample in each experiment.

2.6 Animal studies

All experimental protocols were approved by the Institutional Animal Care and Use Committee (IACUC) of the University of Wisconsin-Madison. Phenotypically normal male mice (heterozygous for *Lepr^{db}*, Jackson Laboratories, Inc.) between the ages of 8-12 weeks were used. Mice were housed in groups during a one week acclimation period prior to the study and housed individually thereafter. Throughout the study period, mice were maintained in a temperature-controlled facility with a standard light/dark cycle. All mice were provided with environmental enrichment and food and water *ad libitum*. Mice were randomly assigned to either control or experimental groups on the day of surgery. For wounding, mice were anaesthetized with inhaled isoflurane, administered using an induction chamber. The mice were injected subcutaneously with buprenorphine (0.1 mg/kg) for pain control and the cranial thoracodorsal region was shaved and aseptically prepared for surgery. Silicone O-rings (McMaster-Carr®, inner diameter 11 mm, outer diameter 15 mm) were applied to the skin 4 mm caudal to the base of the ears on each side of the dorsal midline and secured with tissue glue (Tissumend II) and six 5-0 interrupted nylon sutures. Wounds were centered in the skin circumscribed by the O-ring. A 6-mm biopsy punch was used to create two symmetrical wounds. Each wound was then covered with an 8-mm disc of Biobrane that had been sterilized by UV light for 30 minutes. Sterile non-adherent padding was placed on top of the Biobrane, and the entire construct was covered with Tegaderm™, secured with tissue glue. Mice were recovered from anesthesia on a warming pad. Wounds were photographed using a digital camera and body weights of mice were registered on post-

operative day 1, and every 2-3 days thereafter until the end of the study. Upon completion of the study, mice were killed by intra-peritoneal injection of Beuthanasia®-D (Schering-Plough) solution (0.5 ml/mouse) after induction of anesthesia.

For the duration of the studies, the splints and sutures were monitored daily. Any loss of contact between the splint and skin was repaired with glue. Broken or missing sutures were replaced under anesthesia as described above, and a dose of buprenorphine was administered subcutaneously (0.1 mg/kg) for pain control. Wounds were removed from analysis if two or more sutures were broken or missing within a 24-hour period. Wounds were digitally traced in the photographs and the area calculated using NIH ImageJ software. Wound closure was calculated at each time point as the percentage of the original wound area.

For microbial-burden studies, a bacterial suspension of *S. aureus* in 10 μL PBS was applied topically to the wound and allowed to absorb for 15 minutes before application of Biobrane. After 72 hours, all mice were euthanized and the wounds with the attached Biobrane were excised aseptically with a 6 mm biopsy punch. Wounds and Biobrane were homogenized for 15 minutes in 1 mL PBS. Homogenates were serially diluted in PBS and plated on blood agar. Bacterial quantification was performed for each wound and reported as CFU per cm^2 of the wound surface area. If a wound yielded no bacterial colonies, a value of 1.0 CFU per cm^2 was assigned to it for purposes of statistical analysis. Bacterial counts for the two wounds on each mouse were averaged and the latter used for statistical analysis in each experimental group.

2.7 Statistical analysis

Statistical analysis was performed using SigmaPlot® software (Systat Software, Inc.). All normally distributed data were analyzed by Student's t-test. All non-normally distributed data were analyzed by Mann-Whitney U test. Significance was set at $p< 0.05$.

3. RESULTS and DISCUSSION

3.1 Design and Fabrication of PEMs containing Chlorhexidine

Chlorhexidine acetate is a small molecule antiseptic drug (Mw= 625 g/mol). It is a synthetic cationic bis-guanide with four imine groups (C=NH), six secondary amine groups (C-NH), and two aromatic rings that are chlorinated in the “para” position (**Fig. 1**). Two apparent pKa's have been reported for chlorhexidine: $pKa_1 = 10.3$, for the first two protonations, and $pKa_2 = 2.2$, for the 3rd and 4th protonations [42, 43]. Between pH 4 and 8, chlorhexidine is dicationic (charge of +2.0). We hypothesized that the dicationic charge of the chlorhexidine molecules would facilitate their incorporation into polyelectrolyte multilayers through electrostatic interactions, as has been reported for other cationic small molecules [44].

Our choice of the polymers reported herein for the fabrication of PEMs containing CX was guided by prior knowledge that PEMs consisting of weak polyelectrolytes PAA and PAH can be assembled under conditions that allow growth and proliferation of mammalian fibroblasts cells (mouse NIH 3T3) on their surfaces [31, 45]. In addition, it has been reported that PAA (glass transition temperature, T_g= 106°C) can form diffusion barriers within polymer multilayer films [46], thereby prolonging the release of relatively small molecules from the films [44]. Motivated by these prior studies, we first investigated the incorporation of cationic chlorhexidine molecules between alternating PAH and PAA bilayers (i.e. a ‘tetralayer’ structure of $(PAH/PAA/CX/PAA)_n$). The PEMs were deposited on plasma-cleaned silicon wafers by sequential dipping of the silicon wafers in solutions of PAH (adjusted to pH 7.5), PAA (adjusted to pH 5.5) and CX (pH of ~8.0). The incorporation of CX into the PEMs was confirmed by determining the increase in the ellipsometric thickness of the films. **Fig. 2a** shows that the thickness of a PEM comprised of

$(PAH/PAA/CX/PAA)_m$ increased with the number of 'tetralayers' deposited (m), from 30±1 nm for m=5 to 46±2 nm for m=10, both of which were significantly greater than the thickness of a PEM of $(PAH/PAA)_5$ (14±1 nm). This initial observation suggested that CX contributed to the growth of the $(PAH/PAA/CX/PAA)_n$ film and that it is feasible to deposit polymer multilayers containing CX.

Building from the result obtained above, and motivated by the goal of reducing the complexity of the procedure used to fabricate CX/PEMs, we next explored if successive deposition of anionic PAA and cationic CX would lead to growth of PEMs (i.e. no PAH). To this end, we first deposited a base layer of $(PAH/PAA)_5$ onto a silicon wafer, and subsequently explored the possible formation of CX and PAA multilayers. As shown in **Fig. 2a**, the thickness of a $(PAH/PAA)_5(CX/PAA)_{10}$ film (32±1 nm) was significantly greater than the thickness of a film of $(PAH/PAA)_5$ alone (14±1 nm). Furthermore, the $(PAH/PAA)_5(CX/PAA)_n$ architecture resulted in stable and reproducible film growth up to n=90 bilayers, as shown by the measurements of ellipsometric thicknesses in **Fig. 2b**. Because CX was sequentially deposited during the growth of the multilayers (as one of the structural components), these results suggest that the total drug loading scales with the number of (CX/PAA) bilayers deposited, and thus can be systematically manipulated via control of the number of multilayers deposited. Based on these screening experiments, we focused our subsequent efforts on characterization of PEMs formed from CX and PAA.

Past studies have reported that when cationic small molecules are used to form PEMs, the molecules diffuse into the bulk of the growing multilayer film, while also adsorbing to the growing interface of the film [44, 47]. Thus, in the PEMs fabricated in this study, each subsequent deposition cycle of CX likely leads to both adsorption and absorption of CX. Such a growth regime should result in an exponential growth of film thickness. However, several studies have described the growth of PEMs where at least one polyelectrolyte was thought to diffuse into the PEM [48, 49]. In those experiments, exponential growth of the thickness of the PEMs was observed until a threshold thickness was reached. When the film grew beyond the threshold thickness, the time available for diffusion of the polymers during fabrication was less than the time necessary for the polymers to absorb into the entire thickness of the film via diffusion. A diffusion-limited linear growth curve was observed after that threshold. Inspection of **Fig. 2b** reveals that linear growth of the thickness of the PEMs containing CX was observed after 20 bilayers of (CX/PAA) were deposited, consistent with diffusion-limited penetration of CX into the growing multilayer. A noteworthy implication of this interpretation is that the concentration of diffusive small molecules is expected to be greatest in the diffusion zone of the film (i.e. the outermost regions). In this situation, an initial burst-release of CX followed by a prolonged linear release is predicted, a point we consider below in our measurements of CX release kinetics. Overall, the key result reported above is that that CX/PEMs can be assembled with a $(PAH/PAA)_5(CX/PAA)_n$ architecture such that they grow linearly in thickness with successive depositions of CX and PAA.

As described in the Introduction, we fabricated CX/PEMs on elastomeric PDMS stamps to enable their subsequent transfer onto the wound-contact surfaces of biologic dressings. We recently reported that it is necessary to incorporate microspheres (with diameters of 1-2 μm) into PEMs during their fabrication to achieve the transfer of the PEMs onto soft substrates [34]. Therefore, we sought next to determine if microspheres could be incorporated into CX/PEMs. To this end, a monolayer of negatively charged carboxylate-modified polystyrene (PS) microspheres (2 μm diameter) was adsorbed onto a $(PAH/PAA)_{10.5}$ foundation layer assembled on PDMS sheet. This was followed by deposition of $(PAA/CX)_n$ multilayers over the microspheres, as illustrated in **Fig. 1c**. The incorporation of fluorescently-labeled microspheres into the PEMs enabled fluorescent imaging (**supplementary Fig. 1**) and

confirmation of the integration of the microspheres into the PEMs. We refer to these PEMs as $(PAH/PAA)_{10.5}$(PS-microspheres) $(CX/PAA)_n$ in the remainder of this paper.

3.2 Characterization of the Release Kinetics of Chlorhexidine from PEMs on PDMS stamps

We hypothesized that an optimal CX release profile from PEMs should involve an initial burst release to kill bacteria in the wounds, followed by a sustained zero-order release to prevent re-growth of bacteria. To enable this design, we first determined the bactericidal effect of CX dissolved in solution. To this end, suspensions containing 10^7 CFU of *S. aureus* in 100 μL Hank's balanced salt solution (HBSS) were incubated for 24 h with various concentrations of CX. **Fig. 3** shows that 1.5 μg/mL of CX in solution resulted in a 3 $\log_{10}$ reduction (99.9%) in the viable bacterial counts. These results suggest that to exert antibacterial activity *in vitro*, the PEMs should release ~1.5 μg/mL of CX into the solutions incubated over them.

To facilitate an initial burst release of CX into solution, we introduced a final step into the fabrication of the PEMs. This step involved incubation of PEMs in a chlorhexidine acetate solution for one hour (compared to the 8 min dip time during the PEM fabrication), followed by a single final rinse with water. This procedure was adopted to maximally load CX into the film for rapid diffusive release upon immersion in a physiological environment (i.e. "burst release"). We observed that this procedure led to the release of 0.84±0.05 μg/mL of CX from the $(PAH/PAA)_{10.5}$(PS-microspheres)$(CX/PAA)_{40}$ films in the first 24 h of incubation in PBS buffer, compared to 0.48±0.04 μg/mL of CX released from films not incubated in chlorhexidine solution during the final step of fabrication; i.e. ~70% more CX released (see Methods for assay details).

The CX release profiles of $(PAH/PAA)_{10.5}$(PS-microspheres)$(CX/PAA)_n$ films with n=40 or n=80, assembled on PDMS stamps, are presented in **Fig. 4**. When maintained in PBS solution on a shaker plate at room temperature, the films provided burst release of 0.84±0.05 and 0.98±0.06 μg/cm^2 of their CX payload, respectively, within first 24 h. This was followed by zero-order release of 0.31±0.03 and 0.35±0.04 μg/cm^2/day of CX, respectively, in a relatively linear fashion for the next 7 days. The two sets released a total of 2.69±0.08 and 3.1±0.03 μg/cm^2 of CX, respectively, over 8 days. Interestingly, we note that PEMs with twice the (CX/PAA) bilayers released only 15% more CX over 8 days, even though the PEMs thickness measurements in **Fig. 2** indicate that PEMs with double the number of bilayers have twice the loading of CX.

To determine if CX released by the $(PAH/PAA)_{10.5}$(PS-microspheres)$(CX/PAA)_n$ films into solution was bactericidal, the PEMs were incubated with solutions containing *S. aureus*. Briefly, 6 mm diameter stamps of PDMS supporting the CX/PEMs were incubated in 96-well plates with 100 μL HBSS containing 10^7 CFU of bacteria on a shaker at 37°C. PDMS stamps without PEMs were used as controls. After 24 h of incubation, the bacterial counts in solution were determined by plating on blood agar. It should be noted that, if a 6 mm diameter film (surface area = 0.28 cm^2) releases 1 μg/cm^2 of CX into solution, it generates a concentration of 2.8 μg/mL of CX in 0.1 mL solution. Because 2.0 μg/mL of CX resulted in 5 $\log_{10}$ reduction in the CFUs of *S. aureus* in solution (**Fig. 3**), we predicted that PEMs releasing ~1 μg/cm^2/day of CX (**Fig. 4**) would demonstrate strong bactericidal activity. **Fig. 5** illustrates that $(PAH/PAA)_{10.5}$(PS-microspheres)$(CX/PAA)_n$ films with n=40 and 80 bilayers of (CX/PAA) did, indeed, cause more than 3 $\log_{10}$ and 4 $\log_{10}$ reductions in CFUs of *S. aureus* in solution, respectively. We also note that films with n=10 bilayers of (CX/PAA) resulted in 2.5 $\log_{10}$ reduction in bacterial counts. PEMs without CX (assembled as $(PAH/PAA)_{10.5}$(PS-microspheres)$(PAH/PAA)_{10}$) did not exert any detectable antibacterial activity (data not shown). The release of ~15% more CX from films with n= 80 bilayers of (CX/PAA), than from films with n=40 bilayers (as shown in **Fig. 4)**, might account for the

greater bactericidal activity of the former in **Fig. 5**. We note here that two factors that likely influence the release of cationic small molecule such as CX from the PEMs are: (i) diffusion of unbound CX from the film; and (ii) displacement of CX from the PEM by diffusion of cationic ions into the PEM, thus promoting drug release [47].

The CX release profiles presented in **Fig. 4**, and their antibacterial activity in **Fig. 5**, are interesting in light of studies by Hidalgo et. al. [22] which reported the cytotoxicity of CX solutions towards primary cultures of human dermal fibroblasts cells. In that study, the viability of fibroblasts (determined using a metabolic activity assay) over 24 h was not significantly impacted by CX concentrations of <5 μg/mL in growth media without fetal bovine serum (FBS), or <10 μg/mL in media supplemented with 10% FBS. The same study also documented that cytotoxic concentrations of CX depend on the duration of exposure to CX. Specifically, for 3h and 8h incubation periods, the non-cytotoxic concentration cut-offs for CX were reported to be 25 μg/ml and 10 μg/ml, respectively (in growth media without serum). Inspection of **Fig. 4** and **Fig. 5** reveals that the bactericidal concentrations of CX released by the CX/PEMs over 24 h are under the cytotoxic threshold of 5 μg/mL [22]. Our results, therefore, suggest that localized delivery of low concentrations of CX using PEMs offers the potential advantage of achieving antibacterial activity without cytotoxicity.

3.3 Functionalization of Biologic Wound Dressings

We next investigated the transfer of the CX/PEMs onto the wound-contact surface of a synthetic biologic wound dressing (Biobrane). First, we used fluorescent imaging to confirm transfer of the $(PAH/PAA)_{10.5}$(PS-microspheres)$(CX/PAA)_n$ films from PDMS stamps onto the wound dressing. These experiments were performed using crimson fluorescent (Ext/Em-625/645 nm) microspheres in PEMs to enable imaging [34]. Micrographs in **Fig. 6** show that PEMs were transferred onto the entire wound-contact surface of the dressing, including the silicone backing and the nylon fibers (out of focus, but visible in the image). For reference, micrographs of Biobrane showing the network of autofluorescent nylon fibers (due to bonded collagen; Ext/Em- 488/515 nm) are presented in **supplementary Fig. 2**. Note that the fluorescent micrographs of crimson microspheres in **Fig. 6** were captured under conditions were the nylon fibers generated negligible fluorescence (black, featureless images were obtained in the absence of the crimson microspheres). The conformal transfer of PEMs onto Biobrane is possible because the elasticity of PDMS stamps permits deformation of the stamp around the topographical features of the dressing. Quantitatively, 82 ± 5% (n=10 samples) of the fluorescent area of PDMS sheets was transferred onto Biobrane by stamping. The high magnification micrograph in **Fig. 6b** is provided to permit evaluation of the uniformity of PEM coating at the micrometer-scale. The granularity in the fluorescent image is seen because only the fluorescent microspheres are visible in the image. Overall, these micrographs show that the CX/PEMs can be stamped uniformly onto the wound-contact surface of the biologic dressing.

We further characterized transfer of the CX/PEMs onto the dressing by determining the release kinetics of CX from the functionalized dressing into PBS solution. **Fig. 7** shows that there was an initial burst release of 0.98±0.12 or 1.12±0.14 μg/cm^2 of CX over first 24 h period from $(PAH/PAA)_{10.5}$(PS-microspheres)$(CX/PAA)_n$ films in which n=40 or 80, respectively. This was followed by zero-order release of 0.34±0.02 or 0.42±0.09 μg/cm^2/day of CX, respectively. The total amount of drug released over 8 days was found to be 3.34±0.27 and 4.08±0.35 μg/cm^2 from the two sets, respectively. Qualitatively, the release kinetics were similar to those observed from PEMs on PDMS stamps (compare **Fig. 7** and **Fig. 4)**. There was, however, a ~30% increase in the total amount of CX released into solution from PEMs stamped onto Biobrane, as compared to PEMs on PDMS stamps. We hypothesize that the mechanical stresses involved in the transfer of PEMs onto the wound

dressing may result in local instability and deconstruction of the PEMs around the microspheres [34], and thus contribute to more rapid elution of CX into solution. Overall, the drug release profiles confirm the desired release characteristics - burst release of CX in the first 24 h followed by sustained zero-order release over the next 7 days.

Next, we evaluated the bactericidal activity of CX/PEMs stamped on the wound-contact surface of Biobrane. Punch biopsies (~6 mm diameter) of the functionalized dressing were incubated for 24 h with 100 μL HBSS containing ~10^7 CFU of *S. aureus* in 96-well plates. Unmodified Biobrane, or wells with no substrate, were used as negative controls in each experiment. **Fig. 8** shows that Biobrane stamped with $(PAH/PAA)_{10.5}$(PS-microspheres) $(CX/PAA)_n$ films with n=10 or n=40 bilayers resulted in a 2 $\log_{10}$ decrease in viable bacterial counts, and films with n=80 bilayers resulted in greater than 3 $\log_{10}$ decrease in viable bacteria (compared to unmodified Biobrane). In separate experiments, Biobrane stamped with $(PAH/PAA)_{10.5}$(PS-microspheres)$(PAH/PAA)_{10}$ (i.e. films with no CX) did not exhibit detectable antibacterial activity (data not shown). Bactericidal activity of CX/PEMs on Biobrane, although effective, was less than that observed on PDMS stamps in this *in-vitro* experimental set-up (3 $\log_{10}$ reduction in viable bacteria on Biobrane compared to 4 $\log_{10}$ reduction on PDMS (**Fig. 5**)). This difference could be due to the presence of collagen peptides in Biobrane which improve the proliferation and survival of bacterial cells, and/or bind the cationic CX to reduce its antibacterial efficacy. This hypothesis is supported by **supplementary figure 3**, which shows growth of one to two $\log_{10}$ orders greater counts of *S. aureus* in HBSS supplemented with 5% or 10% FBS than in HBSS with no serum after 24 h incubation at 37°C. Furthermore, increasingly greater concentrations of CX were required (2.0 μg/mL, 3.0 μg/mL or 5.0 μg/mL) to kill *S. aureus* below the detection limit in HBSS containing 0%, 5% and 10% FBS, respectively.

3.4 Efficacy of CX-Functionalized Biobrane Evaluated in Model Dermal-Wounds in Mice

A widely used full-thickness ‘splinted’ dermal wound model in mice, as described elsewhere [50], was adapted for our study. In this wound model, a splint sutured around the wound reduces wound-contracture so that wound closure is primarily by epithelialization. By minimizing wound contraction, this mouse model better mimics human dermal wound healing [50]. Biobrane stamped with $(PAH/PAA)_{10.5}$(PS-microspheres)$(CX/PAA)_{80}$ films was first investigated for its adherence to the wound-bed, and promotion of normal wound healing, as compared to unmodified Biobrane. Two splinted wounds (6 mm diameter) were created on the flanks of each mouse and covered with 8 mm diameter pieces of either unmodified Biobrane (n=10 mice) or with Biobrane stamped with CX/PEMs (n=10 mice). Wounds were photographed (over the transparent Biobrane) on days 0, 3, 7, 10 and 14 after surgery. The epithelial coverage of the wounds was assessed from digital images. As the wounds epithelialized beneath the dressing, Biobrane was released at the edges. The resulting free portion of Biobrane was carefully trimmed from around the edges of the wounds. Adherence of Biobrane was evaluated on a scale of 1 to 4, with a value of 1 assigned to Biobrane not adhered to a wound; value of 4 to Biobrane strongly adhered to the wound-bed; and value of 2 and 3 to Biobrane with intermediate adherence to the wound. Images of two representative wounds under the test dressings on post-operative day 0, 7 and 14 are presented in **Fig. 9**. These images show that wounds treated with CX/PEMs-functionalized Biobrane exhibited similar rates of epithelialization as compared to those treated with unmodified Biobrane, and that both types of dressings remained adherent to the wounds for at least 14 days. No significant difference was observed in the adherence of either type of Biobrane to the wound-bed on days 3, 7, 10 and 14 (n=5 mice, $p>0.05$, Mann-Whitney U-test). **Fig. 9G** summarizes the wound size (presented as % of original wound size) measured on post-operative days 3, 7, 10 and 14 from digital photographs of the wounds. The results indicate that wound closure rates of wounds treated with unmodified

Biobrane, or Biobrane stamped with CX/PEMs, were not significantly different (n≥5 mice, p>0.05, Mann-Whitney U-test). Overall, these results indicate that functionalization of Biobrane with CX/PEMs did not impair or mask the ability of collagen peptides in Biobrane to promote integration into the wound-bed, nor did it impair promotion of normal wound healing under the dressing.

The antimicrobial efficacy of CX-functionalized Biobrane was tested in splinted dermal wounds topically inoculated with ~2×10^5 CFU/cm^2 of *S. aureus*. The wounds were subsequently covered with either unmodified Biobrane, or Biobrane stamped with $(PAH/PAA)_{10.5}$(PS-microspheres) $(CX/PAA)_{80}$ films (n=10 mice for each group). We note here that a bacterial level of 10^5 CFU/g of tissue is equivalent to those isolated from clinically relevant infected wounds [51]. Wounds and dressings were monitored daily. After 3 days of treatment, mice were euthanized, and wounds (along with adherent Biobrane) were excised and homogenized for bacterial quantification. The day 3 time point was used for evaluation because it has been documented that it takes 48-72 h for fibrovascular ingrowth to occur within Biobrane, and allow it to strongly adhere to the wound tissue [35]. If bacterial colonization under Biobrane can be prevented during the first 3 days, it greatly improves the likelihood that the dressing will adhere to the wound and remain so until wound-closure.

Fig. 10 shows that an average of 7.19×10^5 CFU/cm^2 of *S. aureus* were recovered from the wounds treated with unmodified Biobrane, signifying colonization of bacteria in wounds under the dressing within 3 days. In contrast, wounds treated with Biobrane stamped with CX/PEMs had 3 $\log_{10}$ fewer bacteria, with an average of 2.42×10^2 CFU/cm^2 (p<0.005, n=10 mice, Mann-Whitney U test). Moreover, the modified Biobrane demonstrated significantly stronger adherence (median of scale 3) to the wound-bed on day 3, compared to unmodified Biobrane with bacterial colonization in wounds (median of scale 2) (p<0.05, n=10 mice, Mann-Whitney U test). Better adherence means better minimization of dead-space between the dressing and the wound-bed, reducing further chances of bacterial colonization. This experiment was repeated three times, using different batches of CX/PEMs fabricated for each experiment, to validate the reproducibility of PEM fabrication and efficacy on the wound dressing. These results indicate that $(PAH/PAA)_{10.5}$(PS-microspheres)$(CX/PAA)_{80}$ films, when stamped on the wound-contact surface of Biobrane, exert an antibacterial activity in the wound-bed that significantly reduces the wound's bacterial burden and improves adherence of Biobrane to the wound-bed.

4. DISCUSSION

This study presents an approach to control wound microbial burden using CX/PEMs stamped onto the wound-contact surface of biologic dressings that achieve sustained and localized delivery of non-cytotoxic concentrations of the antiseptic chlorhexidine (CX) into wounds. Our study demonstrates that CX/PEMs, when stamped onto a biologic dressing (Biobrane), do not impair the ability of the biologic dressing to adhere to the wound-bed and promote normal wound healing. Significantly, functionalization of the biologic dressing with CX/PEMs prevented colonization of bacteria in wounds under the dressing. The approach reported herein for incorporation of CX in biologic dressings differs from strategies currently used to introduce antibacterial agents into wound dressings. For example, a polyurethane foam dressing impregnated with 25% w/w chlorhexidine gluconate (Biopatch®, Johnson & Jonhson, Somerville, NJ) releases 40 μg/mL/h of CX into water at room temperature, while a hydrogel pad impregnated with 2% w/w chlorhexidine gluconate (Tegaderm-CHG®, 3M HealthCare, St. Paul, MN) releases 240 μg/mL/h of CX [12, 28]. Those dressings clearly release concentrations of CX that exceed the reported *in vitro* cytotoxicity limit of 5 μg/mL for human dermal fibroblasts over 24h [22], thus limiting use of the dressings to skin cleansing around wounds (eg. catheter injection sites). In contrast,

integration of CX/PEMs onto the wound contact surface of biologic dressings allows localized release of CX at the site of potential bacterial colonization (the wound-bed), thus, significantly reducing the loading of CX needed to achieve a useful antimicrobial effect.

We believe that the approach reported here can be broadly applied to localized release of other small cationic molecules and wound modulating factors (antibacterial, analgesics, antibiotics, anti-inflammatory) into wound-beds. We note that a prior study reported immersion of a PEM-coated suture into a CX solution. However, that study did not form multilayers from CX and, nor did they show release of CX from PEMs [52]. Several prior studies have reported incorporation of small drug molecules into PEMs by using prodrugs [53] or preencapsulation [26]. Our approach, in contrast, does not require modification of the active molecule or its encapsulation prior to incorporation into PEMs. We note that there are reports describing impregnation of cationic small molecules such as the antibiotic gentamicin into PEMs, deposited onto the surface of bone implants [44, 47]. In contrast to our study, however, those PEMs were micrometer-thick films, and employed hydrolytically degradable polyelectrolytes to release the impregnated drug as the film degraded. We make note that none of these studies involved the mechanical transfer of preformed PEMs onto wound dressings.

A key element of the approach presented in this study involves stamping pre-fabricated PEMs onto the biologic dressing, thus circumventing the exposure of dressing to harsh chemical processing used in PEMs fabrication. Biologic dressings have not previously been impregnated with antimicrobial agents such as CX because the required processing conditions are incompatible with labile biologic components of the dressings, and would likely compromise the bioactivity and physical structure of the dressings (e.g. dressings containing lyophilized proteins). The methods presented in this study appear suitable for integration of a range of bioactive molecules onto biologic dressings and other tissue substrates. Although we used polystyrene microspheres in this study to transfer CX/PEMs onto the soft biologic dressing, microspheres of biodegradable polymers such as PLGA can also be used [34]. Moreover, PLGA microspheres can potentially serve as reservoirs of bioactive molecules and provide their controlled release as the microspheres hydrolytically degrade [54].

Finally, the wound microbial burden model used in this study is relevant to the clinical use of Biobrane and other biologic dressings, which are not recommended for application to wounds colonized with bacteria [5, 9]. In the biomedical literature, wounds colonized with more than 10^5 CFU/g of tissue are considered microbially infected [51]. That number of bacterial cells will result in non-adherence of Biobrane to the wound and lead to clinical infection under the dressing [5, 6, 9]. We have demonstrated that Biobrane stamped with CX/PEMs results in 3 $\log_{10}$ decrease in the bacterial burden of wounds inoculated with 10^5 CFU/cm^2 of *S. aureus* within 72 h. Clinical guidelines indicate that it takes 48-72 h for Biobrane to adhere to wounds [35]. If Biobrane does not adhere to the wound, infection is likely present [36]. Thus, the results presented in this study suggest that Biobrane stamped with CX/PEMs might be effective on wounds currently viewed as susceptible to microbial colonization during treatment with biologic dressings. We note here that the ‘splinted’ full-thickness wound-model used in this study promotes wound healing primarily by epithelialization, which is relevant to human dermal wounds. Future studies will investigate the use of biologic dressings stamped with CX/PEMs in more clinically relevant, large partial-thickness wounds (in pigs), over longer time periods, and against several pathogenic bacterial strains.

5. CONCLUSION

We demonstrate that integration of CX/PEMs on the wound-contact surface of biologic dressings can provide localized release of non-toxic levels of CX that are effective at reducing the microbial burden of a wound and preventing wound infections under the dressing. This approach achieves a significant reduction in the required loading of CX in the dressing, as compared to currently available CX based formulations and dressings. This study also demonstrates a generalized methodology for using PEMs to incorporate cationic small molecules onto the wound contact surface of biologic dressings, providing precise control over the localization and loading of the bioactive agents. PEMs can be tailored to provide burst release of non-cytotoxic levels of CX followed by sustained zero-order release for another 7 days. By mechanically transferring pre-fabricated PEMs from elastomeric stamps onto soft biologic dressing, exposure of the dressing to harsh chemical processing is avoided. Biobrane stamped with CX/PEMs reduced viable counts of *S. aureus* by 3 $\log_{10}$ in murine wounds inoculated with bacteria, in contrast to microbial colonization observed under unmodified Biobrane. Functionalization of Biobrane with CX/PEMs improved its adherence in wounds inoculated with bacteria. Furthermore, Biobrane stamped with CX/PEMs promoted normal wound healing in mice over 14 days. Overall, this study demonstrates materials and methods for localized delivery of non-toxic concentrations of bioactive agents such as chlorhexidine for *in vivo* wound management. The approaches can potentially be used to functionalize the surfaces of a range of biological tissues and implantable devices to improve their clinical performance.

Supplementary Material

Refer to Web version on PubMed Central for supplementary material.

Acknowledgments

The authors thank Kathleen M. Guthrie, Kevin W. Johnson, Dana S. Tackes, and Allison R. Clarke for assistance with mice studies, Nancy G. Faith for help with antibacterial experiments, and undergraduate students Gladys V. Roldan Rivera and Winny Budiman for assistance in fabrication/characterization of PEMs. The funding for this study was provided by NIH grant 1RC2AR058971-01 from NIAMS and an Innovation & Economic Development Research grant from the University of Wisconsin-Madison Graduate School. A.A. acknowledges fellowship support from the Ewing Marion Kauffman Foundation.

REFERENCES

1. Rizzi SC, Upton Z, Bott K, Dargaville TR. Recent advances in dermal wound healing: Biomedical device approaches. Expert Rev Med Devices. 2010; 7:143–54. [PubMed: 20021245]
2. Shores JT, Gabriel A, Gupta S. Skin substitutes and alternatives: A review. Adv Skin Wound Care. 2007; 20:493–508. [PubMed: 17762218]
3. Kearney JN. Clinical evaluation of skin substitutes. Burns. 2001; 27:545–51. [PubMed: 11451613]
4. Nichols KG, Moaveni Z, Mcewan C, Alkadhi A, Mcewan W, Alkadhi A. BA01 Audit of Waikato regional burns centre: Biobrane infection rates. ANZ J Surg. 2009; 79:A7–A.
5. Ou LF, Lee SY, Chen YC, Yang RS, Tang YW. Use of Biobrane in pediatric scald burns-experience in 106 children. Burns. 1998; 24:49–53. [PubMed: 9601591]
6. Gonce S, Miskell P, Waymack JP. A comparison of Biobrane vs. Homograft for coverage of contaminated burn wounds. Burns. 1988; 14:409–12.
7. Prasad JK, Feller I, Thomson PD. A prospective controlled trial of Biobrane versus Scarlet Red on skin graft donor areas. J Burn Care Res. 1987; 8:384–6.
8. Lang EM, Eiberg CA, Brandis M, Stark GB. Biobrane in the treatment of burn and scald injuries in children. Ann Plast Surg. 2005; 55:485–9. [PubMed: 16258299]

9. Lal S, Barrow RE, Wolf SE, Chinkes DL, Hart DW, Heggers JP, et al. Biobrane improves wound healing in burned children without increased risk of infection. Shock. 2000; 14:314–9. [PubMed: 11028549]
10. Echague C, Hair P, Cunnion K. A comparison of antibacterial activity against methicillin-resistant staphylococcus aureus and gram-negative organisms for antimicrobial compounds in a unique composite wound dressing. Adv Skin Wound Care. 2010; 23:406–13. [PubMed: 20729646]
11. Bhende S, Rothenburger S. In vitro antimicrobial effectiveness of 5 catheter insertion-site dressings. J Assoc Vasc Access. 2007; 12:227–31.
12. Bhende S, Spangler D. In vitro assessment of chlorhexidine gluconate impregnated polyurethane foam antimicrobial dressing using zone of inhibition assays. Infect Cont Hosp Ep. 2004; 25:664–7.
13. Wu SC, Crews RT, Zelen C, Wrobel JS, Armstrong DG. Use of chlorhexidine-impregnated patch at pin site to reduce local morbidity: The chipps pilot trial. Int Wound J. 2008; 5:416–22. [PubMed: 18205786]
14. Beighton D, Decker J, Homer KA. Effects of chlorhexidine on proteolytic and glycosidic enzyme activities of dental plaque bacteria. J Clin Periodontol. 1991; 18:85–9. [PubMed: 2005230]
15. Gendron R, Grenier D, Sorsa T, Mayrand D. Inhibition of the activities of matrix metalloproteinases 2, 8, and 9 by chlorhexidine. Clin Diagn Lab Immunol. 1999; 6:437–9. [PubMed: 10225852]
16. Gomes BPFA, Souza SFC, Ferraz CCR, Teixeira FB, Zaia AA, Valdrighi L, et al. Effectiveness of 2% chlorhexidine gel and calcium hydroxide against enterococcus faecalis in bovine root dentine in vitro. Int Endod J. 2003; 36:267–75. [PubMed: 12702121]
17. Fraser JF, Bodman J, Sturgess R, Faoagali J, Kimble RM. An in vitro study of the antimicrobial efficacy of a 1% silver sulphadiazine and 0.2% chlorhexidine digluconate cream, 1% silver sulphadiazine cream, and a silver coated dressing. Burns. 2004; 30:35–41. [PubMed: 14693084]
18. Kumar RJ, Kimble RM, Boots R, Pegg SP. Treatment of partial-thickness burns: A prospective, randomized trial using transcytetm. ANZ J Surg. 2004; 74:622–6. [PubMed: 15315558]
19. Ruschulte H, Franke M, Gastmeier P, Zenz S, Mahr K, Buchholz S, et al. Prevention of central venous catheter related infections with chlorhexidine gluconate impregnated wound dressings: A randomized controlled trial. Ann Hematol. 2009; 88:267–72. [PubMed: 18679683]
20. Giannelli M, Chellini F, Margheri M, Tonelli P, Tani A. Effect of chlorhexidine digluconate on different cell types: A molecular and ultrastructural investigation. Toxicol In Vitro. 2008; 22:308–17. [PubMed: 17981006]
21. Faria G, Cardoso CRB, Larson RE, Silva JS, Rossi MA. Chlorhexidine-induced apoptosis or necrosis in l929 fibroblasts: A role for endoplasmic reticulum stress. Toxicol Appl Pharm. 2009; 234:256–65.
22. Hidalgo E, Dominguez C. Mechanisms underlying chlorhexidine-induced cytotoxicity. Toxicol In Vitro. 2001; 15:271–6. [PubMed: 11566548]
23. Decher G. Fuzzy nanoassemblies: Toward layered polymeric multicomposites. Science. 1997; 277:1232–7.
24. Boudou T, Crouzier T, Ren K, Blin G, Picart C. Multiple functionalities of polyelectrolyte multilayer films: New biomedical applications. Adv Mater. 2011; 22:441–67. [PubMed: 20217734]
25. Su X, Kim B-S, Kim SR, Hammond PT, Irvine DJ. Layer-by-layer-assembled multilayer films for transcutaneous drug and vaccine delivery. ACS Nano. 2009; 3:3719–29. [PubMed: 19824655]
26. Smith RC, Riollano M, Leung A, Hammond PT. Layer-by-layer platform technology for small-molecule delivery. Angew Chem Int Ed Engl. 2009; 48:8974–7. [PubMed: 19847838]
27. Rossi S, Marciello M, Sandri G, Ferrari F, Bonferoni MC, Papetti A, et al. Wound dressings based on chitosans and hyaluronic acid for the release of chlorhexidine diacetate in skin ulcer therapy. Pharm Dev Technol. 2007; 12:415–22. [PubMed: 17763146]
28. Karpanen TJ, Casey AL, Conway BR, Lambert PA, Elliott TSJ. Antimicrobial activity of a chlorhexidine intravascular catheter site gel dressing. J Antimicrob Chemoth. 2011; 66:1777–84.
29. Van Den Plas D, De Smet K, Lens D, Sollie P. Differential cell death programmes induced by silver dressings in vitro. Eur J Dermatol. 2008; 18:416–21. [PubMed: 18573715]

30. Trop M, Novak M, Rodl S, Hellbom B, Kroell W, Goessler W. Silver-coated dressing acticoat caused raised liver enzymes and argyria-like symptoms in burn patient. J Trauma. 2006; 60:648–52. [PubMed: 16531870]
31. Agarwal A, Weis TL, Schurr MJ, Faith NG, Czuprynski CJ, McAnulty JF, et al. Surfaces modified with nanometer-thick silver-impregnated polymeric films that kill bacteria but support growth of mammalian cells. Biomaterials. 2010; 31:680–90. [PubMed: 19864019]
32. Park J, Hammond PT. Multilayer transfer printing for polyelectrolyte multilayer patterning: Direct transfer of layer-by-layer assembled micropatterned thin films. Adv Mater. 2004; 16:520–5.
33. Kohli N, Worden RM, Lee I. Intact transfer of layered, bionanocomposite arrays by microcontact printing. Chem Commun. 2005; 289:316–8.
34. Agarwal A, Guthrie KM, Czuprynski CJ, Schurr MJ, McAnulty JF, Murphy CJ, et al. Polymeric multilayers that contain silver nanoparticles can be stamped onto biological tissues to provide antibacterial activity. Adv Funct Mater. 2011; 21:1863–73.
35. Tavis MJ, Thornton JW, Bartlett RH, Roth JC, Woodroof EA. A new composite skin prosthesis. Burns. 1980; 7:123–30.
36. Greenwood JE, Clausen J, Kavanagh S. Experience with Biobrane: Uses and caveats for success. Eplasty. 2009; 9:243–55.
37. Skaife JJ, Abbott NL. Quantitative characterization of obliquely deposited substrates of gold by atomic force microscopy: Influence of substrate topography on anchoring of liquid crystals. Chem Mater. 1999; 11:612–23.
38. Brake JM, Abbott NL. An experimental system for imaging the reversible adsorption of amphiphiles at aqueous-liquid crystal interfaces. Langmuir. 2002; 16:6101–9.
39. Gupta JK, Tjipto E, Zelikin AN, Caruso F, Abbott NL. Characterization of the growth of polyelectrolyte multilayers formed at interfaces between aqueous phases and thermotropic liquid crystals. Langmuir. 2008; 24:5534–42. [PubMed: 18419143]
40. Lockwood NA, Cadwell KD, Caruso F, Abbott NL. Formation of polyelectrolyte multilayer films at interfaces between thermotropic liquid crystals and aqueous phases. Adv Mater. 2006; 18:850–4.
41. Ostad SN, Gard PR. Cytotoxicity and teratogenicity of chlorhexidine diacetate released from hollow nylon fibres. J Pharm Pharmacol. 2000; 52:779–84. [PubMed: 10933128]
42. Gadde RR, McNiff EF, Peer MM. High-performance liquid chromatographic analysis of chlorhexidine phosphanilate, a new antimicrobial agent. J Pharmaceut Biomed. 1991; 9:1031–6.
43. Hugo WB, Longworth AR. Some aspects of the mode of action of chlorhexidine. J Pharm Pharmacol. 1964; 16:655–62. [PubMed: 14226440]
44. Moskowitz JS, Blaisse MR, Samuel RE, Hsu H-P, Harris MB, Martin SD, et al. The effectiveness of the controlled release of gentamicin from polyelectrolyte multilayers in the treatment of staphylococcus aureus infection in a rabbit bone model. Biomaterials. 2010; 31:6019–30. [PubMed: 20488534]
45. Mendelsohn JD, Yang SY, Hiller J, Hochbaum AI, Rubner MF. Rational design of cytophilic and cytophobic polyelectrolyte multilayer thin films. Biomacromolecules. 2003; 4:96–106. [PubMed: 12523853]
46. SalomaÌ, Mk; Kankare, J. Influence of synthetic polyelectrolytes on the growth and properties of hyaluronanâ^'chitosan multilayers. Biomacromolecules. 2009; 10:294–301. [PubMed: 19119871]
47. Chuang HF, Smith RC, Hammond PT. Polyelectrolyte multilayers for tunable release of antibiotics. Biomacromolecules. 2008; 9:1660–8. [PubMed: 18476743]
48. Porcel C, Lavalle P, Ball V, Decher G, Senger B, Voegel JC, et al. From exponential to linear growth in polyelectrolyte multilayers. Langmuir. 2006; 22:4376–83. [PubMed: 16618190]
49. Porcel C, Lavalle P, Decher G, Senger B, Voegel JC, Schaaf P. Influence of the polyelectrolyte molecular weight on exponentially growing multilayer films in the linear regime. Langmuir. 2007; 23:1898–904. [PubMed: 17279672]
50. Robert DG, Joseph M, Michael D, Jamie PL, Geoffrey CG. Quantitative and reproducible murine model of excisional wound healing. Wound Repair Regen. 2004; 12:485–92. [PubMed: 15260814]
51. Robson MC, Mannari RJ, Smith PD, Payne WG. Maintenance of wound bacterial balance. Am J Surg. 1999; 178:399–402. [PubMed: 10612536]

52. Harnet J-C, Le Guen E, Ball V, Tenenbaum H, Ogier J, Haikel Y, et al. Antibacterial protection of suture material by chlorhexidine-functionalized polyelectrolyte multilayer films. J Mater Sci: Mater Med. 2009; 20:185–93. [PubMed: 18709445]

53. Thierry B, Kujawa P, Tkaczyk C, Winnik FM, Bilodeau L, Tabrizian M. Delivery platform for hydrophobic drugs: Prodrug approach combined with self-assembled multilayers. J Am Chem Soc. 2005; 127:1626–7. [PubMed: 15700982]

54. Mohamed F, van der Walle CF. Engineering biodegradable polyester particles with specific drug targeting and drug release properties. J Pharma Sci. 2008; 97:71–87.

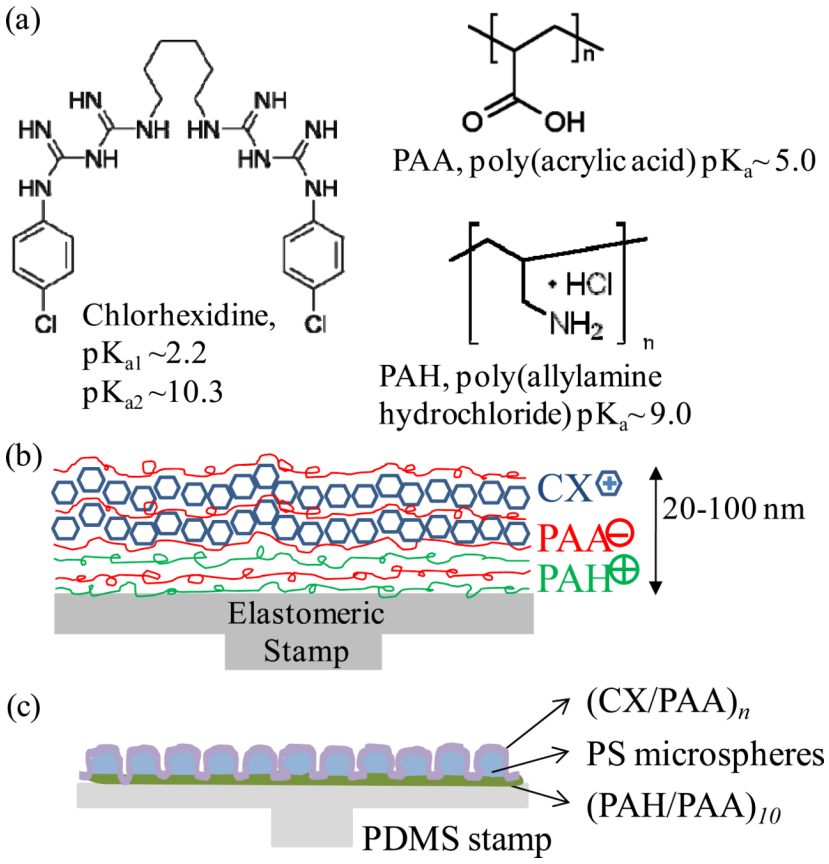

Figure 1.

(a) Molecular structures of polyelectrolytes and the chlorhexidine (CX) used in the fabrication of PEMs; (b) schematic illustration of polymer multilayers of $(PAH/PAA)_5(CX/PAA)_n$ assembled by layer-by-layer deposition, and (c) schematic illustration of the films containing $(PAH/PAA)_{10.5}$(PS microspheres)$(CX/PAA)_n$, prepared on elastomeric PDMS stamps.

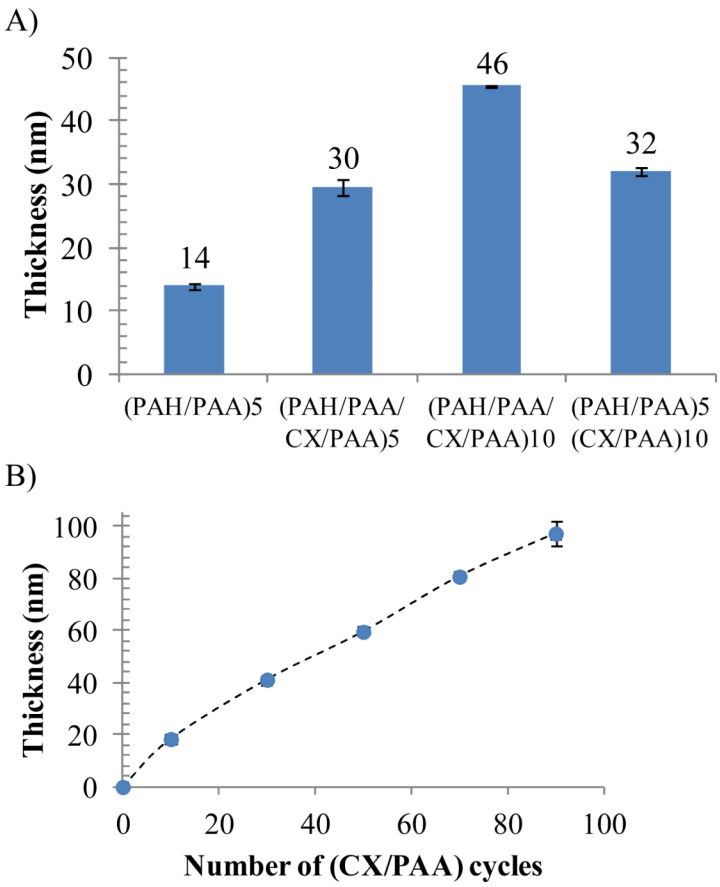

Figure 2.

Ellipsometric thicknesses of PEMs assembled on the native oxide surface of silicon wafers. (A) Cumulative thickness of PEMs with the structure $(PAH/PAA/CX/PAA)_n$ or $(PAH/PAA)_5(CX/PAA)_{10}$, both assembled on the native oxide surface of silicon wafers (B) Cumulative thickness of PEMs of $(CX/PAA)_n$ deposited on a foundation of $(PAH/PAA)_5$. Thickness of only $(CX/PAA)_n$ is plotted. Data represent the mean ± standard deviation ($n \geq 4$).

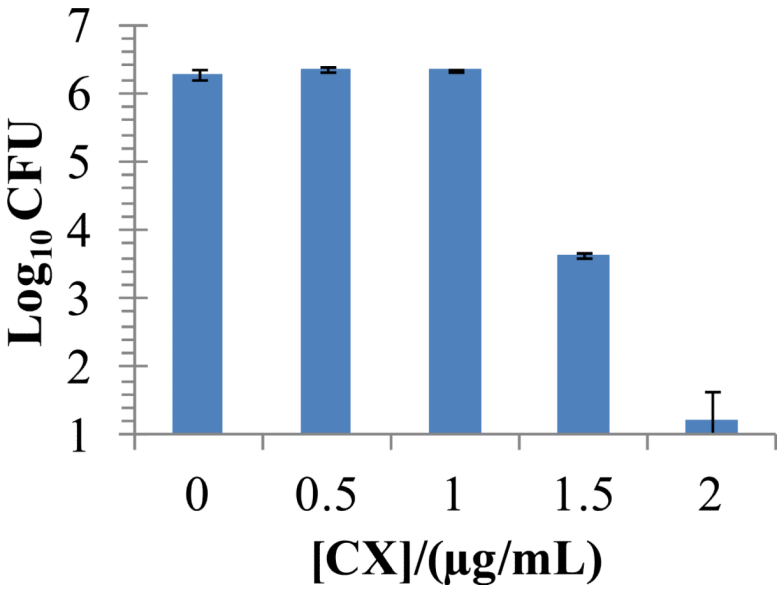

Figure 3.
Dose-dependent antibacterial activity of chlorhexidine acetate solutions against S. aureus in HBSS buffer over 24 h incubation at 37°C. Data represent the mean ± SEM (n≥4) from one representative experiment that was repeated three times.

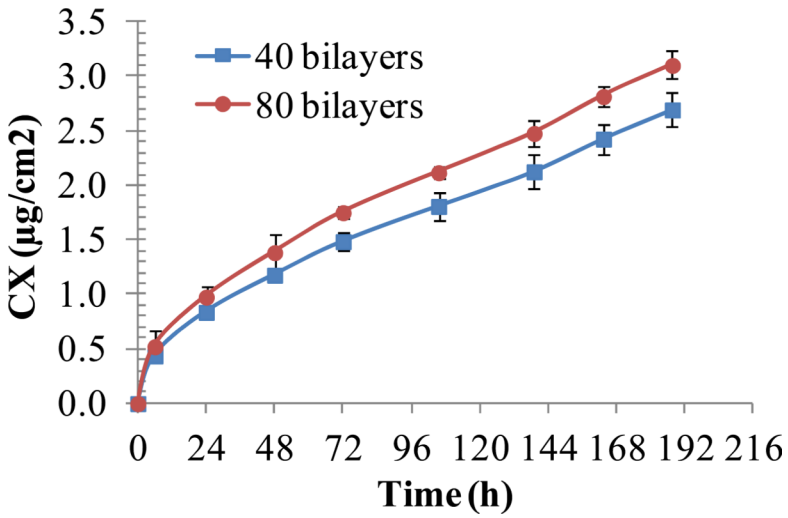

Figure 4.

Cumulative release of CX into PBS solution from PEMs of $(PAH/PAA)_{10.5}$(PS microspheres)$(CX/PAA)_n$, with n=40 or 80, assembled on PDMS stamps. PEMs (2 cm diameter) were incubated in PBS and concentration of eluted CX was measured by UV-vis spectroscopy. Data represent the mean ± standard deviation (n=3) from one representative experiment that was repeated with three different batches of PEMs.

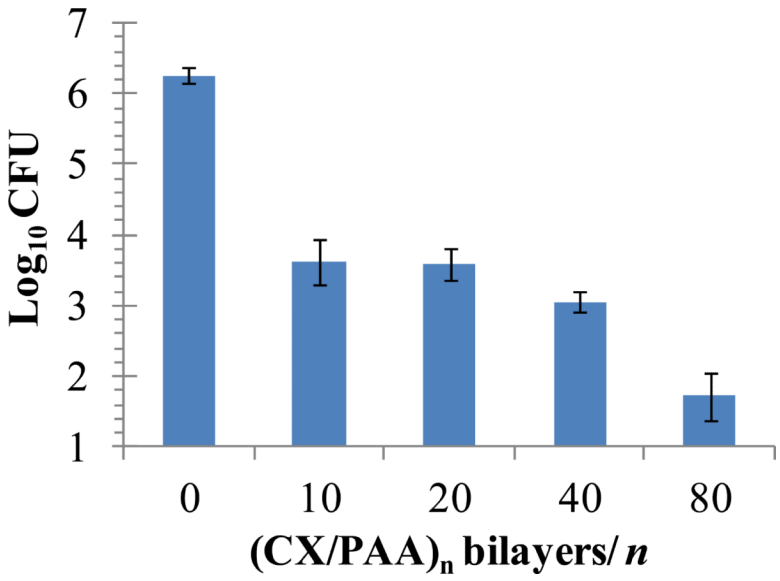

Figure 5.

Colony Forming Units (CFU) of *S. aureus* recovered in HBSS solution incubated over $(PAH/PAA)_{10}$(PS microspheres)$(CX/PAA)_n$ films, assembled on PDMS stamps, for 24 h at 37°C. These data illustrate that antibacterial activity was dependent on the number of (CX/PAA) bilayers in the films. Data represent the mean ± SEM ($n \geq 4$) from one representative experiment that was repeated three times.

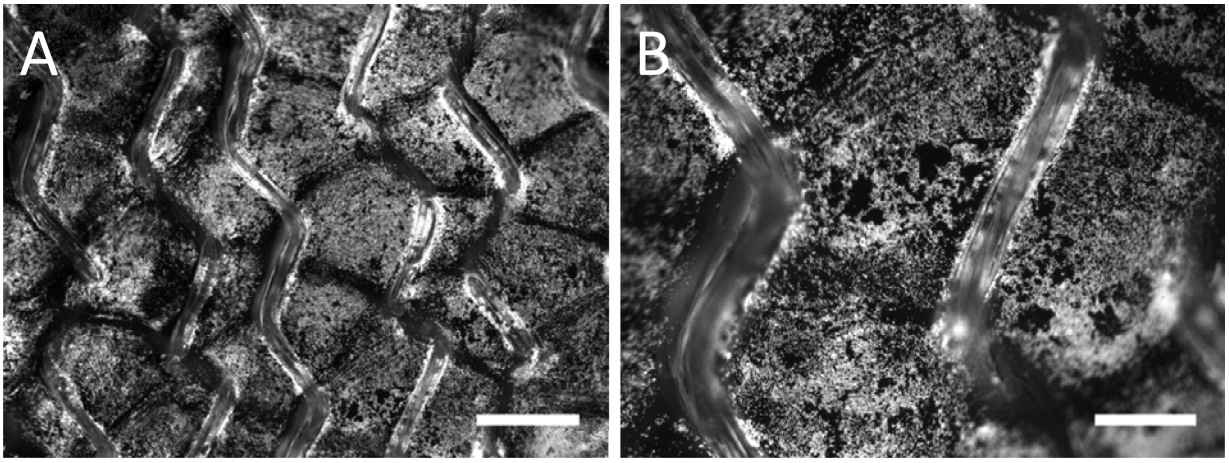

Figure 6.

Representative fluorescent micrographs of $(PAH/PAA)_{10}$(PS microspheres) $(CX/PAA)_{40}$ films stamped onto the wound-contact surface of Biobrane. The fluorescence is from crimson-fluorescent polystyrene (PS) microspheres embedded in the PEMs. (A) Low magnification image. Scale bar=500 μm; (B) High magnification image. Scale bar= 200 μm.

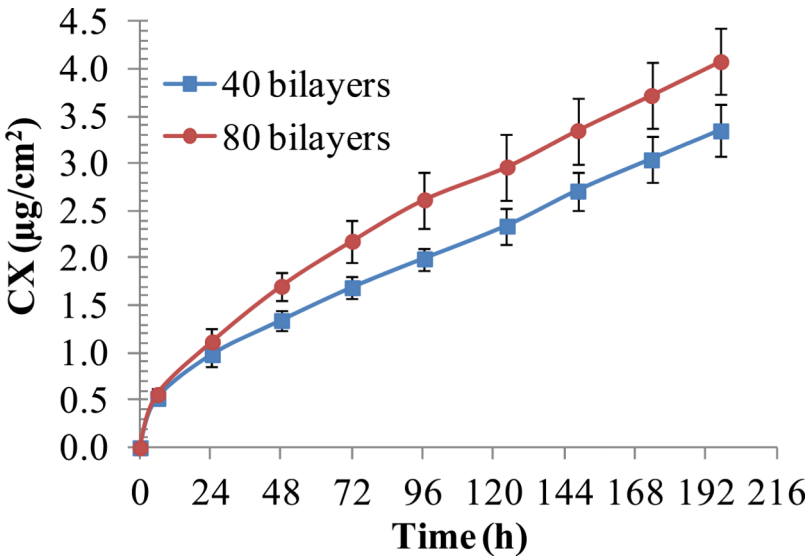

Figure 7.

Effect of $(CX/PAA)_n$ bilayers on the cumulative release of CX into PBS buffer from $(PAH/PAA)_{10}$(PS microspheres)$(CX/PAA)_n$ films, with n=40 or 80, stamped on the Biobrane wound dressing. Data represent the mean ± standard deviation (n=3) from one representative experiment that was repeated with three different batches of PEMs.

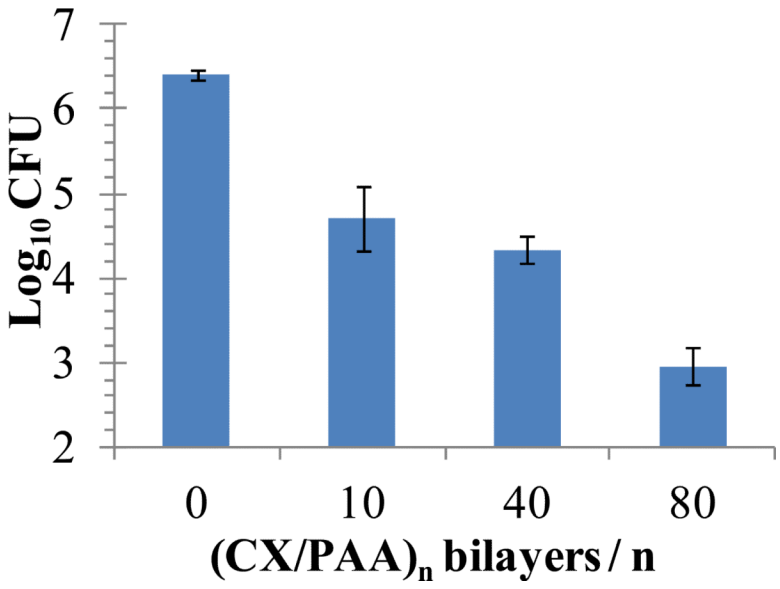

Figure 8.

Colony Forming Units (CFU) of *S. aureus* recovered from buffer solutions incubated over (PAH/PAA)$_{10}$(PS microspheres)(CX/PAA)$_n$ films, stamped onto the Biobrane wound dressing, for 24 h at 37°C. Antibacterial activity of the functionalized dressing was dependent on the number of (CX/PAA) bilayers in the films. Data represent the mean ± SEM ($n \geq 4$) from one representative experiment that was repeated three times.

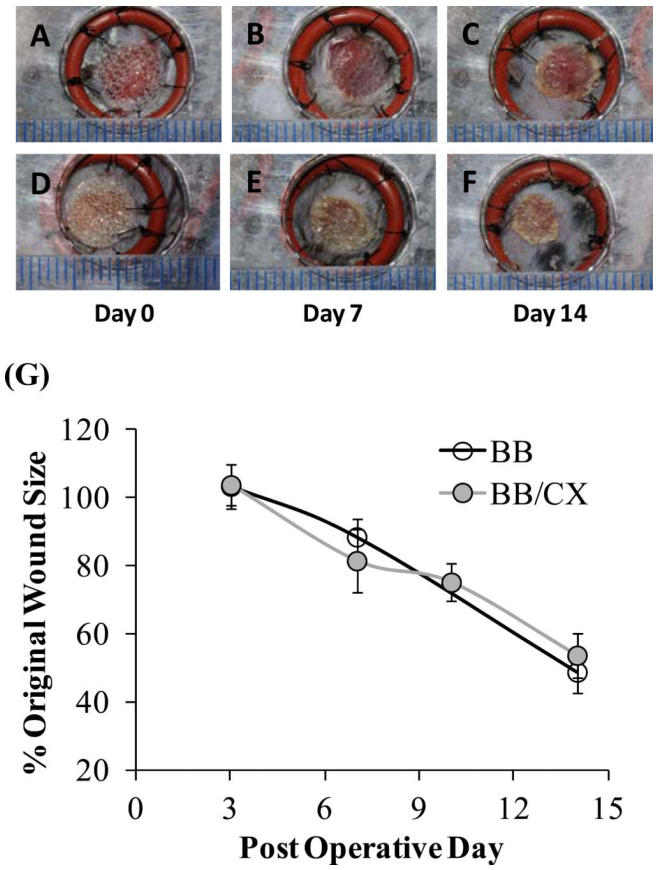

Figure 9.

Biobrane functionalized with CX/PEMs promoted normal healing in 'full-thickness' splinted dermal wounds (6 mm diameter) in normal wild-type mice. Digital images showing simple, gross observation of wound healing on post-operative days 0, 7 and 14, respectively, in groups treated with: (A, B, C) Biobrane, or (D, E, F) Biobrane functionalized with PEMs of $(PAH/PAA)_{10}$(PS microspheres)$(CX/PAA)_{80}$. (G) Percentage of original wound size on post-operative days 3, 7, 10 and 14 in groups treated with either Biobrane functionalized with CX/PEMs, or unmodified Biobrane. Each data point presents mean ± SEM of relative wound size ($n \geq 5$ mice). Results show that CX/PEMs do not impair the adherence of the dressing to the wounds (as seen from gross images), nor the rate of wound closure.

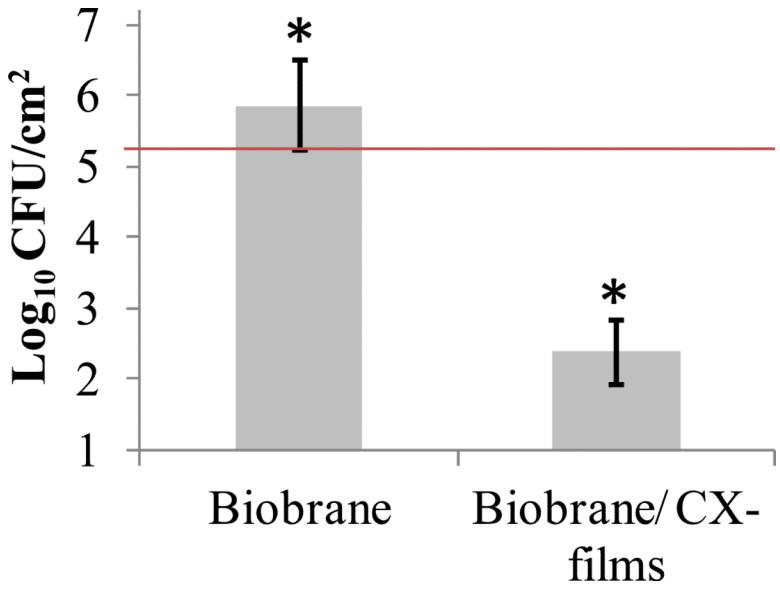

Figure 10.

Colony Forming Units (CFU) of *S. aureus* recovered from 'full-thickness' dermal wounds (in normal wild-type mice) inoculated with 2.1×10^5 CFU/cm^2 of *S. aureus* (illustrated by horizontal line) and treated for 3 days with either Biobrane functionalized with PEMs of $(PAH/PAA)_{10}(PS\text{-microspheres})(CX/PAA)_{80}$, or unmodified Biobrane ($p<0.05$, $n=10$ mice per group, Mann-Whitney U test). Data represent the mean ± SEM from one representative experiment that was repeated three times. Results show that CX/PEMs resulted in 3 $\log_{10}$ reduction in the wound microbial burden under the Biobrane.